A Combined High Temperature Tape-Casting and 2D Freeze-Casting Method for Polymer Membranes with Vertically Oriented Pores

Thesis by
Mahi Gokuli

In Partial Fulfillment of the Requirements for the
Degree of
Bachelor of Science in Materials Science

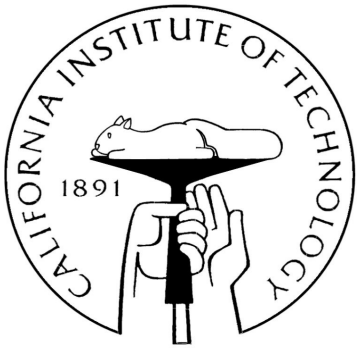

CALIFORNIA INSTITUTE OF TECHNOLOGY
Pasadena, California

2021
Defended May 28, 2021

Mahi Gokuli
ORCID: 0000-0001-9771-826X

ACKNOWLEDGEMENTS

Thank you to my advisor, Dr. Faber, and Vince Wu, for their guidance and mentorship, and for the opportunity to conduct part of my thesis in the laboratory amidst COVID-19 restrictions.

I would also like to thank the entire Faber group; Ben Herren, Celia Chari, Laura Quinn, Sara Gorske, Kevin Yu, and Zane Taylor; for their insights and support during group meetings.

Lastly, I would like to thank my family, close friends, prior mentors, professors, and TAs for their support during my time at Caltech.

ABSTRACT

Alternatives to lithium-ion batteries often require novel electrolytes, such as solvent-in-salt electrolytes and ionic liquids, for which commercial battery separators are unsuited. The Faber Lab at Caltech is researching processing methods for separators made of polymer/ceramic composite materials to ensure high wettability in novel liquid electrolytes. To this end, a flexible polymer separator is needed which provides a short working-ion transportation path for high ionic conductance. Here, a method was developed for the fabrication of poly(vinylidene fluoride-co-hexafluoropropylene) (PVDF-HFP) membranes with vertically aligned, nontortuous pores with pore diameters of a few microns by directional crystallization of dimethyl sulfone ($DMSO_2$). The method combines high-temperature tape casting and bidirectional freeze casting into a single step. Important considerations for the improvement of the method (particularly, avenues for reducing the pore size to below 1 μm) are discussed. In addition, the role of PVDF-HFP crystallization in bidirectional freeze-casting, a solvent crystallization method, is discussed.

TABLE OF CONTENTS

LIST OF ILLUSTRATIONS

LIST OF TABLES

Chapter 1

INTRODUCTION

Lithium-ion batteries have revolutionized portable electronics and are currently the technology of choice for most electric vehicles. They are also a contender for use in grid-scale energy storage systems to balance the intermittency of renewable energy sources. Estimates of future battery demand vary widely and must take into account these coming developments, as well as policy interventions and other emerging technologies. Growing markets for lithium-ion batteries raise concerns about whether raw materials supply will be able to meet demand in the near future. In addition to conceivable challenges in rapidly scaling up production of lithium and cobalt (which is used to increase cathode energy density), the geographic concentrations of cobalt mining and refinement also present geopolitical risks [8]. Lastly, safety issues such as fires and explosions limit the applications of lithium-ion batteries. Recently, there has been a demand for new battery chemistries which have greater raw material abundance and high energy density. Potential alternatives to lithium-ion batteries include halogen conversion-intercalation chemistry, Mg-ion, and particularly Na-ion batteries, which may be a cost-effective solution for stationary and household-based renewable energy storage [5].

These new battery chemistries often require novel electrolytes due to differences in operating voltage, working ions, solvation environments, and charge transport requirements [5]. Novel liquid electrolytes such as "solvent in salt" electrolytes and ionic liquids are able to meet these requirements while improving the ionic conductivity, cation transference number, and cycling stability of the batteries [5]. In sodium-ion batteries, ionic liquids were found to provide higher sodium-ion transference number and improved rate performance and cycling lifetime [5]. Water-in-salt electrolytes have also been demonstrated in sodium-ion batteries [5]. For lithium based batteries, ionic liquids have garnered attention because of their non-flammability, negligible vapor pressure, high thermal and electrochemical stabilities, as well as smooth lithium plating and stripping capabilities [5]. In aqueous lithium-ion batteries, water-in-salt electrolytes have expanded the electrochemical stability window to 3 to 4 volts, allowing high voltage cathodes to be coupled with low voltage graphite anodes and even enabling use of halogen conversion-intercalation

chemistry [5] [10]. In summary, these novel liquid electrolytes show potential to enable safer alternatives to lithium-ion batteries, with enhanced rate performance and cycle life.

An essential component of battery cells is the separator, which mechanically separates the anode and cathode but is still permeable to the working ions which travel between them. Compatibility (wettability) between the separator and the electrolyte enables the working ions to easily pass through the separator pores, lowering the internal resistance of the battery. Due to the variability of viscosity with temperature and varying hydrophobic/hydrophilic nature of highly concentrated electrolytes, finding a separator compatible with novel liquid electrolytes is challenging [5]. Incompatibility with commercial separators is the main barrier preventing the use of novel liquid electrolytes in batteries; furthermore, the use of commercial separators in gauging the potential of new battery chemistries is complicated and limiting [5].

The Faber Lab at Caltech is researching processing methods for separators made of polymer/ceramic composite materials in order to ensure high wettability in novel liquid electrolytes, with vertically aligned, non-tortuous submicron pores for increased ionic conductance. The vertically aligned pores are achieved using a bidirectional freeze-casting process. This project will focus on exploring and improving bidirectional freeze-casting methods for various polymer-solvent systems to obtain polymer separators with the proper pore morphology and size. Additional considerations for the separators (which are beyond the scope of this project) include ensuring high wettability in novel liquid electrolytes, sufficient mechanical strength, flexibility, and thermal and electrochemical stability. The development of these separators will enable the advancement of battery technologies which have the potential to be a safer, more sustainable alternative to lithium-ion batteries.

Chapter 2

BACKGROUND

2.1 Current Separators for Novel Liquid Electrolytes

Even as ionic liquids and solvent-in-salt electrolytes show great promise for new battery chemistries, they face the hurdle of incompatibility with commercial separators. Commercial separators for lithium-ion batteries are commonly made of polyolefin polymers, which have poor wettability in concentrated electrolytes. In the past, glass fiber separators, non-woven fabric separators, and polymer separators coated with ceramic or inorganic particles have been used as alternatives to commercial polyolefin separators [5]. However, these solutions come with their own challenges, which are outlined below. Here, the Macmullin number N_m is used to describe the effect of the separator on the conductivity of the assembly (electrolyte and separator). The MacMullin number is the ratio of the resistivity of the assembly to that of the electrolyte alone; a higher MacMullin number therefore means lower ionic conductivity.

1. **Glass fiber separators:** Glass fiber separators have a very low MacMullin number ($N_m \sim 1$), as well as high wettability and porosity, making them ideal for evaluating the properties of novel liquid electrolytes. However, due to their large, open pore structure, they must be relatively thick (> 300 μm) to prevent short-circuiting of the battery, which is impractical for applications. Furthermore, their brittleness prevents them from being rolled into the jelly-roll configuration used in cylindrical battery cells.

2. **Non-woven fabric separators:** Electrospun polyacrylonitrile (PAN) microfiber separators have a relatively low MacMullin number ($N_m \sim 5$), though it is still five times that of a glass-fiber separator. The increase in resistivity is likely because of the low wettability of the PAN microfibers compared to glass. In addition, their large, open pore structure necessitates them to be relatively thick (> 200 μm), making them unsuitable for practical applications.

3. **Polymer separators coated with ceramic or inorganic particles:** Two such commercial separators exist: polyolefin separators coated with inorganic

particles (Celgard®), and polyethylene terephthalate (PET) separators coated with ceramic particles (Separion®). These separators have been shown to have increased wettability in several ionic liquid electrolytes compared to uncoated polyolefin separators. However, Celgard® and Separion® separators have high MacMullin numbers ($N_m > 25$ and $N_m \sim 10$, respectively), likely because of the low wettability of polymer layer in the substrate and the tortuous nature of their pores.

The aim of the research at the Faber Lab is to develop processing methods for a flexible separator compatible with novel liquid electrolytes with a low MacMullin Number ($N_m < 3$) and standard thickness (~ 25 μm). This may be achieved by (1) using a polymer-ceramic composite material (with ceramic fillers incorporated throughout the separator, rather than only as a coating on the surface) to increase the wettability of the separator in the electrolyte, and (2) using a bidirectional freeze-casting method to create a separator with vertically aligned, non-tortuous submicron pores, thereby providing a short working-ion transportation path to ensure high ionic conductance and preventing the need for high thickness.

2.2 Background on Polymeric Membrane Fabrication

2.2.1 Phase Separation Methods

The most common fabrication method for polymeric membranes is phase inversion, due to its versatility and scalability [2]. In this process, the polymer-solvent solution undergoes demixing, separating into a polymer-rich and polymer-lean phase [2]. The solvent is then removed to form a solid membrane [2]. The dominant method to fabricate polymeric membranes using phase inversion is nonsolvent-induced phase separation (NIPS) [2]. In this method, the polymer is dissolved in solvent, cast into a film, and then immersed into a nonsolvent bath to induce phase separation [2]. Phase inversion by NIPS therefore requires an understanding of the interactions between the polymer, solvent, and nonsolvent. Another method for phase inversion is thermally-induced phase separation (TIPS), in which the polymer of interest is dissolved in solvent at an elevated temperature, cast into a film, and cooled to induce phase separation [2]. Phase inversion by TIPS therefore requires consideration of the polymer-solvent interaction, cooling rate, and thermal gradient. One advantage of the TIPS method is that membranes may be fabricated from semicrystalline polymers that are usually insoluble in solvents at ambient temperatures [2].

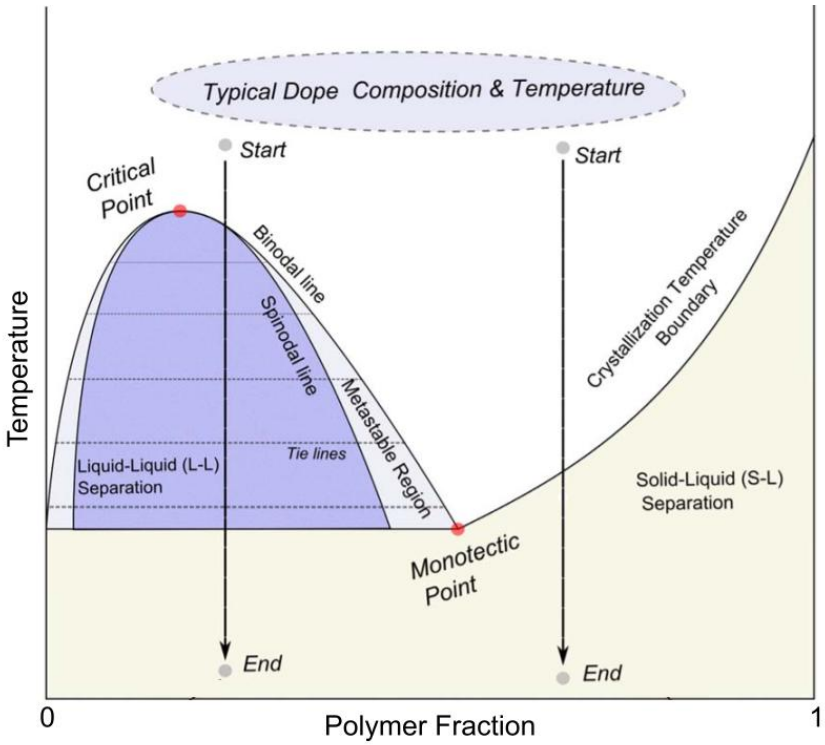

Figure 2.1: Diagram of TIPS process [2]. The two arrows show the paths of low and high polymer concentration dope solutions upon cooling, leading to cellular and spherulitic membrane morphologies, respectively.

The TIPS process is represented by the diagram shown in Figure 2.1 [2]. The two arrows in Figure 2.1 are used to show the path followed by two stable dope solutions with low and high polymer concentrations being cooled from a high temperature. Upon cooling, the low polymer concentration solution phase separates into a polymer-poor phase and a polymer-rich phase along the tielines, before ultimately passing through the crystallization temperature boundary, when the polymer-poor phase becomes the pores of the membrane, while the polymer-rich phase becomes the membrane. This process gives a cellular morphology. For the high polymer concentration solution, the membrane passes directly through the crystallization temperature boundary, and solid-liquid phase separation occurs and the polymer crystallizes directly from the dope solution. This process gives a spherulitic morphology [2].

2.2.2 Crystallization Methods

In contrast to phase separation methods, crystal habit is a key consideration in crystallization methods [1]. In directional freeze-casting, at least one temperature

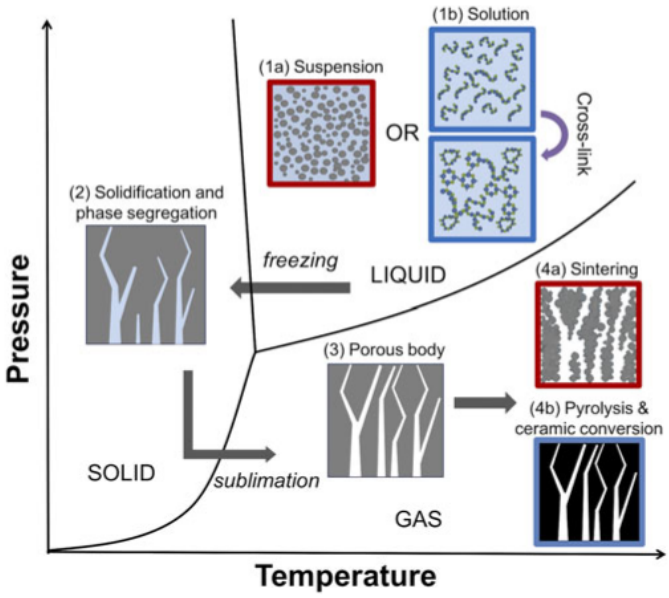

Figure 2.2: Phase diagram of the freeze-casting process [7].

gradient is used to induce the directional crystallization of solvent molecules. The solvent crystals are then removed by sublimation, resulting in a membrane with low tortuosity, oriented pores. This process can be observed in steps 1 through 3 of the phase diagram in Figure 2.2. In unidirectional freeze-casting, a single temperature gradient is imposed, generally by placing the suspension on a cold finger, so that the solvent crystals nucleate randomly on the cold finger surface [5]. This results in high variation in the pore size and crystal orientation, making it difficult to scale up the fabrication of consistent, uniformly-oriented structures using this method [5].

In bidirectional freeze-casting, two perpendicular temperature gradients are imposed on the suspension to prevent the solvent crystals from nucleating randomly on the cold surface [4]. Instead, oriented nucleation occurs, with a freezing front travelling in the direction of the second temperature gradient (Figure 2.3) [4]. Compared to unidirectional freeze-casting, this method results in greater uniformity in the size and shape of the pores [5].

Two methods for bidirectional freeze casting found in the literature are shown in Figures 2.4 and 2.5. In the setup shown in Figure 2.4, the suspension is placed in between a glass slide and a stainless steel plate, then placed into cold water bath (Figure 2.4) [4]. The first temperature gradient arises from the difference in thermal conductivity between stainless steel and glass: the stainless steel plate cools faster than the glass plate, so that the crystals grow directionally from the stainless steel

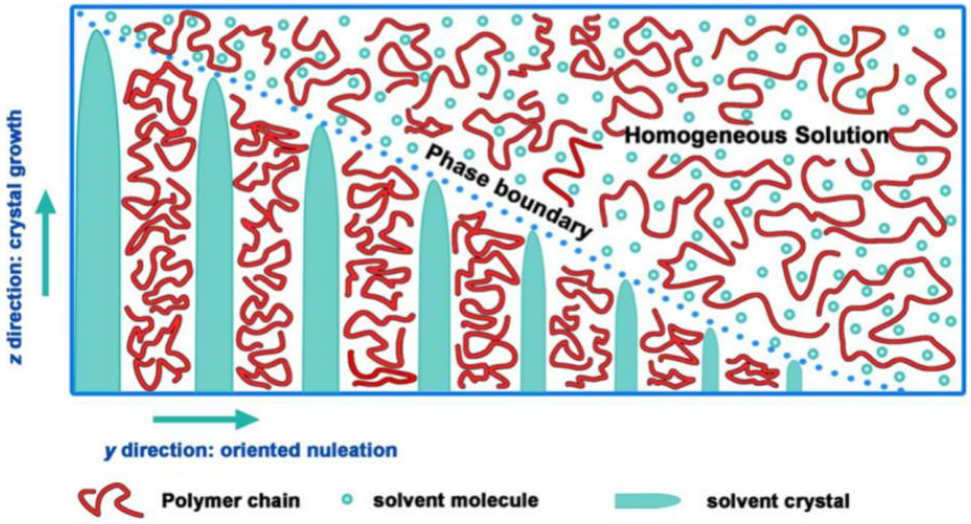

Figure 2.3: Oriented nucleation and crystal growth resulting from a dual thermal gradient [4].

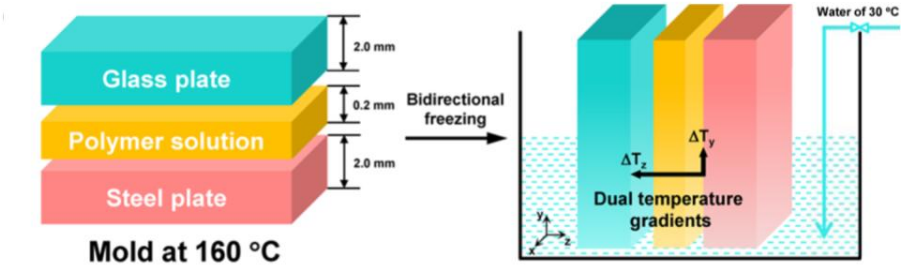

Figure 2.4: Glass-steel sandwiching method for bidirectional freeze-casting [4].

to glass plate [4]. The second (much smaller) thermal gradient comes from the addition of coolant (water) into the reservoir [4]. As a result, the solvent crystals will begin nucleating at the bottom of the bath, and the freezing front will travel towards the top of the bath as the water level rises [4].

In the setup shown in Figure 2.5, the suspension is tape-cast onto a wafer which is moved at a fixed rate towards a liquid nitrogen reservoir [1]. The two temperature gradients arise from the position of the sample relative to the liquid nitrogen reservoir; the solvent crystals grow directionally from the wafer to the free end of the membrane, while the freezing front travels away from the liquid nitrogen reservoir. This method is particularly useful for solvents with a low melting point.

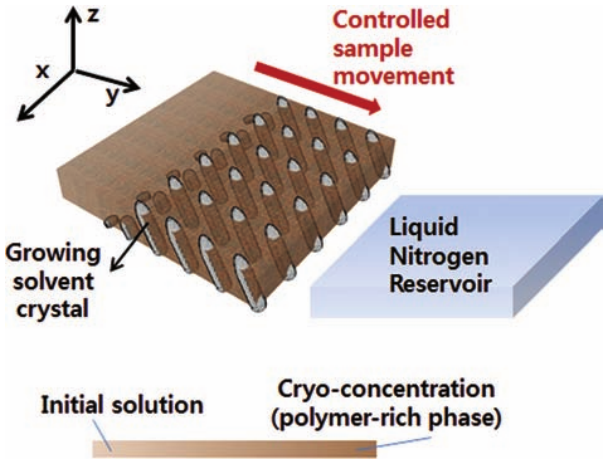

Figure 2.5: LN_2 reservoir method for bidirectional freeze casting [1].

2.2.3 Polymer-Solvent Systems

Polyvinylidene fluoride (PVDF) is a widely used membrane material because of its thermal stability, chemical inertness, low flammability, and excellent mechanical properties. Its copolymer, poly(vinylidene fluoride-co-hexafluoropropylene) (PVDF-HFP) has increased solubility and mechanical strength, with the tradeoff of higher hydrophobicity.

One promising polymer-solvent system is PVDF-HFP in dimethyl sulfoxide (DMSO) and 1,4-dioxane cosolvents. Using the bidirectional freeze-casting method shown in Figure 2.5, Kim et al. obtained membranes with high porosity and pores of low tortuosity by using DMSO and 1,4-dioxane cosolvents to restrict solvent crystallization [1]. Using this method, they were able to control pore size over a wide range, from several tens of microns to a few hundred nanometers [1]. In particular, a 1:1 mixture of the cosolvents yielded a reduced pore size of up to a few hundred nanometers [1]. Furthermore, titania nanoparticles were able to be introduced into PVDF solution during the freeze-casting step, resulting in ceramic nanoparticles being successfully dispersed in a nanocomposite membrane without sacrificing the pore structure [1]. One consideration for this method is that while the thermodynamic melting points of dioxane and DMSO are 11.8°C and 19°C, respectively, in the 1:1 cosolvent mixture the restricted crystallization depresses the melting point by more than 50°C, making a low temperature freeze-casting method such as the one shown in Figure 2.5 necessary [1].

Another promising polymer-solvent system is PVDF-HFP in dimethyl sulfone ($DMSO_2$). Since $DMSO_2$ has a melting temperature of 109°C, the suspension preparation and

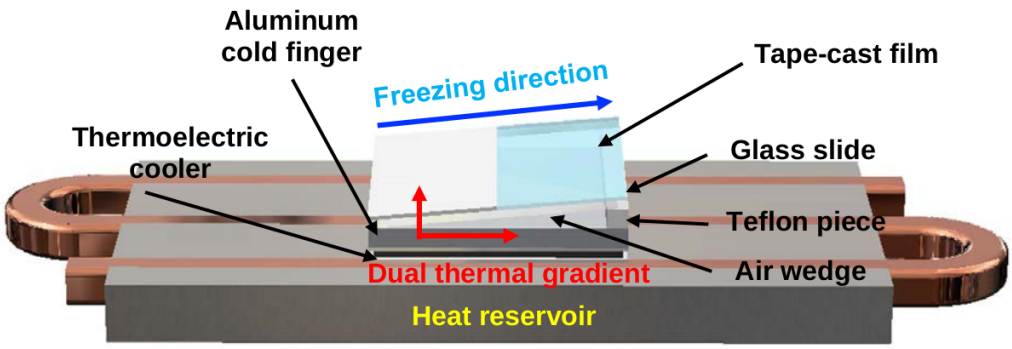

Figure 2.6: Air wedge method for bidirectional freeze casting [9].

tape casting must take place above this temperature. Using the method shown in Figure 2.4 (while pre-heating the mold), Liang et al. obtained membranes with vertically aligned, through-thickness micron-scale pores [4]. Using the TIPS method (Section 2.2.1), they were able to dissolve higher weight percentages (up to 30%) of PVDF in $DMSO_2$ while maintaining a cellular pore morphology, and by doing so were able to achieve a much higher tensile strength ($\sim$ 8 MPa) [3]. In contrast, in the PVDF-HFP in dioxane system, a maximum of 20 wt% of PVDF-HFP could be dissolved. Lastly, Liang et al. found that 88.9% of $DMSO_2$ could be recovered when extracted by sublimation, making it an eco-friendly option [3].

2.3 Prior Work on Separators the Faber Lab

2.3.1 Bidirectional Freeze-Casting Method

A third method for bidirectional freeze casting was developed at the Faber Lab. Here, the suspension is tape-cast onto a glass slide, which is then positioned on top of an aluminum cold finger such that one end of the slide is in contact with the cold finger and the other end rests on a Teflon spacer (Figure 2.6). The slope of the air wedge relative to the cold finger imposes two temperature gradients on the suspension simultaneously. As a result, the pore-forming crystals begin nucleating at the bottom of the wedge and grow outwards away from the cold finger, and the freezing front travels upwards along the wedge. The solvent is then extracted, resulting in the porous membrane.

2.3.2 Polymer-Solvent Systems

Through-thickness, directionally aligned pores with pore diameter on the scale of 5 μm to 10 μm were obtained using the method from Section 2.3.1 (Figure 2.6) using 15 wt% PVDF-HFP in dioxane [9]. In addition, ball milling was used to disperse

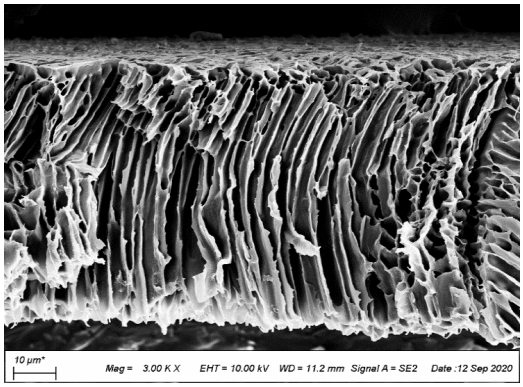

Figure 2.7: Membrane prepared from PVDF-HFP in $DMSO_2$ [9].

alumina particles into the suspension before it was tape and freeze-cast [9]. Up to 15 wt% alumina (with respect to the PVDF-HFP) was thoroughly incorporated this way without sacrificing the microstructure [9]. The incorporation of alumina was shown to improve the thermal stability of the membranes and lead to less thermal shrinkage upon heating [9]. Infiltration was also used to incorporate silica into the polymer membrane [9]. This was performed after the suspension was tape-cast and freeze-cast into a porous membrane structure [9]. The membrane was infiltrated with tetraethyl orthosilicate (TEOS) and then subjected to sol-gel processing, allowing nano-sized silica particles to become embedded into the pore walls [9]. The addition of either ceramic filler (alumina or silica) into the membrane was shown to increase the tensile strength by 25% to 30% from pure PVDF-HFP membranes [9].

The goals for this project build upon the previous work done at the Faber Lab. The pore size obtained in membranes made with 15 wt% PVDF-HFP in dioxane is not sufficiently small. The first goal is to explore a method to fabricate membranes with smaller pores using cosolvents, following the work done by Kim et al. (Section 2.2.3). Due to the melting point depression of the cosolvent mixture, a method for low-temperature freeze casting will have to be designed to investigate the cosolvent method. In addition, the use of $DMSO_2$ as a solvent gave a promising preliminary result, with vertically aligned, smaller pores (on the scale of 1 μm to 3 μm) (Figure 2.7) [9]. However, due to the high melting temperature of $DMSO_2$ (109°C), the tape casting for this membrane was performed by hand inside of an oven. The second goal is to continue exploring this polymer-solvent system by designing a safer setup for high-temperature tape-casting.

Chapter 3

METHODS

3.1 PVDF-HFP Membranes Prepared in $DMSO_2$

PVDF-HFP membranes were prepared in the solvent $DMSO_2$. Since $DMSO_2$ has a melting temperature of 109°C, the suspension preparation and tape casting must take place above this temperature. The tape casting therefore took place on top of an aluminum block placed inside of a silicone oil bath (Figure 3.1), which was heated to the desired temperature outlined in Table 3.1. The glass slide onto which the membrane was tape-cast and the tape-casting knife were also pre-heated by resting on top of the aluminum block. This setup was used rather than a hot plate to ensure greater temperature uniformity across the membrane during tape-casting.

To prepare the membranes, PVDF-HFP (in pellet form) and $DMSO_2$ (in powder form) were added to a vial in the amounts listed in Table 3.1. The vial was closed and placed inside of a silicone oil bath on top of a stirring hot plate at 160°C. Once the PVDF-HFP pellets and $DMSO_2$ were sufficiently melted, a small stir bar was added and set to >300 rpm. The stir bar cannot be added earlier due to the viscous nature of the mixture. Once the PVDF-HFP pellets were well dissolved, the temperature was reduced to the tape-casting temperature listed in Table 3.1 and the frequency of the stir bar was reduced to 50 rpm until all small bubbles were dispelled. The mixture was then put onto a glass slide, where it was tape and freeze-cast into a membrane.

At this point, the procedure differed between samples. Firstly, while initial samples were tape-cast at 160°C, for later samples 130°C was found to be sufficient. The temperatures used to tape-cast each sample are given in Table 3.1. Secondly, various methods were tested for tape casting and freeze casting the membrane. These are also outlined in Table 3.1 and described as follows. In Method 1, the tape-casting knife was pulled backwards over the entire slide while the slide was held in a fixed position; then, the sample was freeze-cast by pushing the slide forwards onto a room temperature steel plate (Figure 3.1a). In Method 2, the position of the tape-casting knife was fixed at the edge of the heated aluminum block, and the sample was tape and freeze-cast by pushing the slide forward underneath the tape-casting knife and

directly onto the room temperature steel plate (Figure 3.1b). This allowed for more uniform tape casting and minimized the evaporation of $DMSO_2$ out of the sample, since the PVDF-$DMSO_2$ mixture remained pooled behind the casting knife until just before being tape-cast and immediately transferred to the steel plate. In Method 3, the position of the tape-casting knife was fixed at the center of the heated aluminum block so that the slide remained on top of the block as it passed underneath the tape-casting knife. After all of the slide had passed under the tape-casting knife, the sample was freeze-cast by pushing the glass slide onto the room temperature steel plate (Figure 3.1c). In Method 4, the tape-casting knife was again fixed at the center of the heated aluminum block. After all of the slide had passed under the knife, the sample was freeze-cast by pushing the glass slide onto the room temperature aluminum block (Figure 3.1d). The aluminum block was used to increase the thermal gradient, since aluminum has a higher thermal conductivity than steel.

After freeze-casting, the membranes were placed in a room temperature water bath overnight, then removed and washed with ethanol before being left to dry in air for 24 hours. The membranes were then cut so that their cross-sections could be imaged using scanning electron microscopy (SEM). This was done by immersing them in liquid nitrogen until they were brittle and applying pressure with a pre-chilled razor blade.

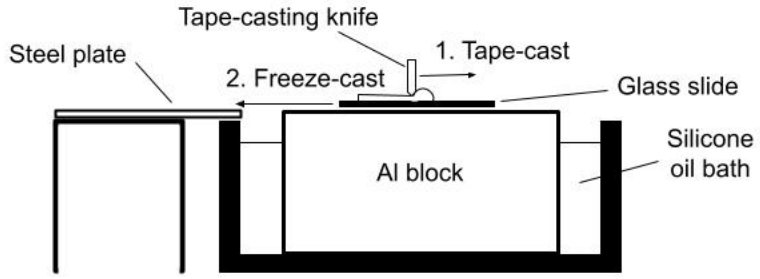

(a) Method 1. The tape-casting knife is pulled over the slide which is in a fixed position, then the slide is pushed onto the steel plate.

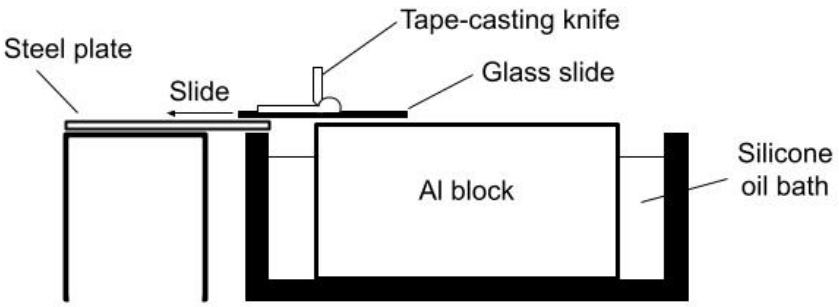

(b) Method 2. The slide is pushed underneath the tape-casting knife, which is fixed at the edge of the aluminum block, onto the steel plate.

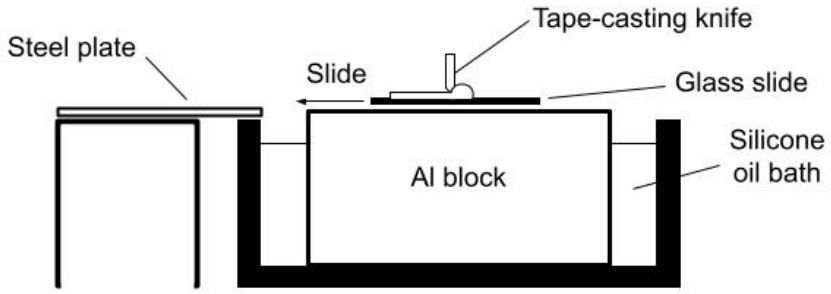

(c) Method 3. The slide is pushed underneath the tape-casting knife, which is fixed at the center of the aluminum block, onto the steel plate.

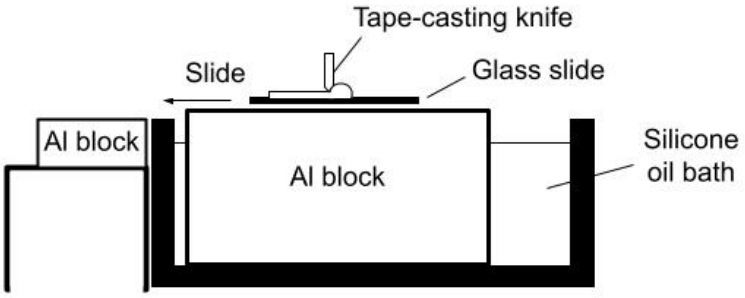

(d) Method 4. The slide is pushed underneath the tape-casting knife, which is fixed at the center of the aluminum block, onto a colder aluminum block.

Figure 3.1: High temperature tape-casting setups (Methods 1-4).

3.2 PVDF-HFP Membranes Prepared in DMSO and Dioxane Cosolvents

PVDF-HFP membranes were prepared by dissolving 15 wt% PVDF-HFP in 7:3 (by weight) and 1:1 (by weight) DMSO:dioxane cosolvents. While the thermodynamic melting points of DMSO and dioxane are 19°C and 11.8°C, respectively, the melting point depression of the cosolvent mixture must be accounted for when

Table 3.1: PVDF-HFP Membranes Prepared in $DMSO_2$

Sample	PVDF-HFP (g)	$DMSO_2$ (g)	Temperature (°C)	Method
1	1.0251	4.1178	160	1
2	1.0199	4.0807	160	1
3	1.0342	4.1369	130	1
4	0.9938	3.9813	130	2
5	1.0115	4.0585	130	2
6	1.0096	4.0328	130	3
7	1.0141	4.0571	130	3
8	1.0375	4.1494	130	3
9	1.0123	4.0481	130	4
10	0.9777	3.9133	130	4

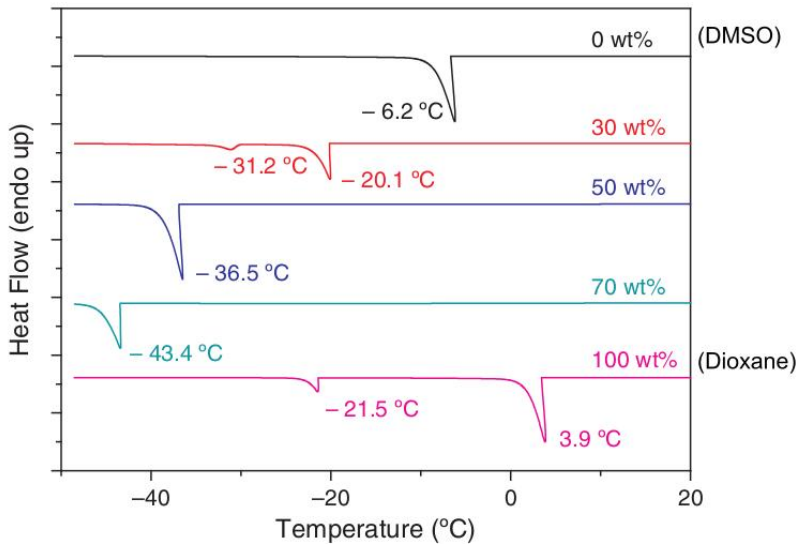

Figure 3.2: DSC thermograms showing crystallization of DMSO and dioxane co-solvents upon cooling in PVDF solutions with different dioxane concentrations [1].

freeze casting the samples. Figure 3.2 shows the crystallization temperatures for various DMSO:dioxane cosolvent ratios in 7 wt% PVDF [1]. Two crystallization temperatures exist because dioxane has two monoclinic crystalline phases, Phase I and Phase II (DMSO only has one monoclinic stable phase) [1]. In pure dioxane, Phase I exists between 5°C and 12°C, and Phase II exists from below -140°C to 5°C [1]. For these experiments, the higher temperature peak corresponding to the crystallization of Phase I was used as the melting temperature. Two different methods which took into account the different melting temperatures were used to freeze-cast the samples.

Table 3.2: PVDF-HFP Membranes Prepared in DMSO and Dioxane Cosolvents

Sample	DMSO:Dioxane	PVDF-HFP (g)	DMSO (g)	Dioxane (g)	Melting Temperature (°C)	Method
11	7:3	0.7770	3.0907	1.3309	-20.1	5
12	1:1	0.7730	2.2014	2.1908	-36.5	6

For each sample, PVDF-HFP (in pellet form), dioxane (in liquid form), and DMSO (in liquid form) were added to a vial in the amounts listed in Table 3.2. DMSO was added last and the vial was quickly closed to minimize evaporation. The vial was sealed with electrical tape to prevent water from leaking into the vial. The vial was then placed in a 70°C water bath on top of a stirring hot plate. After the PVDF-HFP had sufficiently melted, the vial was removed from the water bath, quickly dried off, and a stir bar was added to the mixture before the vial was re-sealed and placed back into the water bath. The mixture was stirred at about 300 rpm until the PVDF-HFP pellets were thoroughly dissolved. The stir rate was then lowered to about 50 rpm until all small bubbles were dispelled. The mixture was then put onto a glass slide and tape-cast on top of a room temperature platform. The tape casting was done by pulling the tape-casting knife backwards over the entire slide while the slide was held in a fixed position.

At this point, the freeze-casting methods diverged due to the differences in melting temperature of the cosolvent mixtures. The methods used for each sample are outlined in Table 3.2. In Method 5, the sample was placed on top of an aluminum cold finger at -25°, such that one end of the slide rested on the cold finger and the other rested on a Teflon spacer (Figure 3.3a). In Method 6, the sample was placed inside an aluminum boat, such that one end of the slide rested on the bottom of the boat and the other rested on a Teflon spacer (Figure 3.3b). The boat was then lowered into a liquid nitrogen bath until it came into contact with the surface (Figure 3.3b). As the boat was being lowered into the liquid nitrogen bath, the temperature of the boat was observed to remain above the required freezing temperature of -36.5°C until the boat was in contact with or very nearly in contact with the liquid nitrogen.

After freeze-casting, the membranes were placed in a -30°C methanol bath overnight and then washed with fresh methanol twice before being left to dry in air for 24

hours. The membranes were then cut so that their cross-sections could be imaged using SEM. This was done by immersing them in liquid nitrogen until they were brittle and applying pressure with a pre-chilled razor blade.

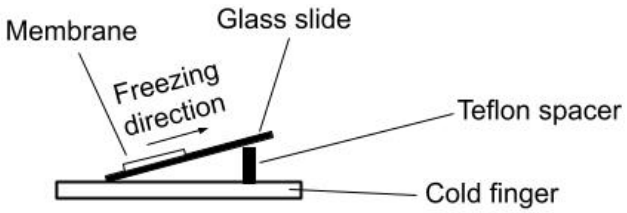

(a) Method 5. One end of the slide rests on a Teflon spacer, while the other is in contact with the aluminum cold finger.

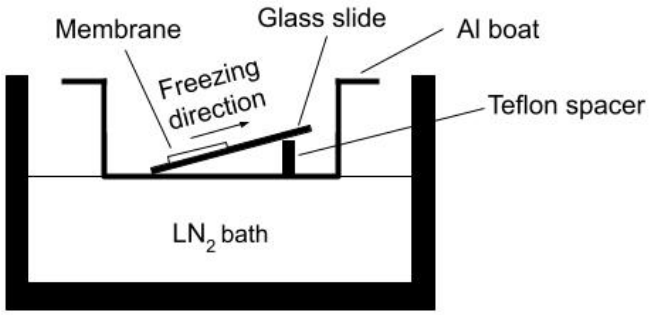

(b) Method 6. One end of the slide rests on a Teflon spacer, while the other is in contact with the floor of an aluminum boat, which is lowered onto a liquid nitrogen bath.

Figure 3.3: Low temperature freeze-casting setups (Methods 5 & 6.)

3.3 PVDF-HFP Membranes Prepared in DMSO and $DMSO_2$ Cosolvents

PVDF-HFP membranes were prepared by dissolving 20 wt% PVDF-HFP in 1:1 DMSO:$DMSO_2$ cosolvents. The melting temperatures of DMSO and $DMSO_2$ are 19°C and 109°C, respectively. With the addition of DMSO, the melting point of $DMSO_2$ was depressed to lower than 70°C. The melting point of the 1:1 cosolvent mixture was found to be between 20°C and 70°C. The cosolvent was prepared first, by adding the $DMSO_2$ (in powder form) followed by the DMSO (in liquid form) to a glass vial in the amounts listed in Table 3.3. The DMSO was added last to minimize evaporation. The vial was quickly closed and sealed with electrical tape, then placed in a 70°C water bath until the $DMSO_2$ had dissolved. The vial was then removed from the bath, dried off, and the PVDF-HFP (in pellet form) was quickly added before the vial was re-sealed and placed once again in the water bath. After

Table 3.3: PVDF-HFP Membranes Prepared in DMSO and $DMSO_2$ Cosolvents

Sample	PVDF-HFP (g)	DMSO (g)	$DMSO_2$ (g)	Steel plate
13	1.0026	2.0149	2.0037	Room temperature
14	1.0090	2.0007	2.0002	Pre-chilled in LN_2

the PVDF-HFP had sufficiently dissolved, the vial was again removed from the bath, dried off, and a stir bar was quickly added to the mixture before the vial was re-sealed and placed again in the bath. The mixture was stirred at about 300 rpm until the PVDF-HFP pellets were thoroughly dissolved. The stir rate was then lowered to about 50 rpm until all small bubbles were dispelled. The mixture was then put onto a glass slide and tape-cast. The samples were tape-cast using Method 3 from Section 3.1 (Figure 3.1d), in which the tape-casting knife was fixed at the center of the aluminum block, which was heated to 70°C in this case. At this point, the methods for freeze casting the samples diverged. One of the samples was freeze-cast using a room temperature steel plate, while the other was freeze-cast using a steel plate that was pre-chilled in liquid nitrogen. After freeze-casting, the membranes were placed in a room temperature water bath overnight, then removed and washed with ethanol twice before being left to dry in air for 24 hours. The membranes were then cut so that their cross-sections could be imaged using SEM. This was done by immersing them in liquid nitrogen until they were brittle and applying pressure with a pre-chilled razor blade.

3.4 PVDF-HFP Membranes Prepared in DMSO

PVDF-HFP membranes were prepared by dissolving 20 wt% PVDF-HFP in DMSO. The melting temperature of DMSO is 19°C, so tape casting was performed at room temperature. To prepare the membranes, PVDF-HFP (in pellet form) and DMSO (in liquid form) were added to a vial in the amounts listed in Table 3.4. The vial was sealed with electrical tape to prevent water from leaking into the vial. The vial was then placed in a 70°C water bath on top of a stirring hot plate. After the PVDF-HFP had sufficiently melted, the vial was removed from the water bath, quickly dried off, and a stir bar was added to the mixture before the vial was re-sealed and placed back into the water bath. The mixture was stirred at about 300 rpm until the PVDF-HFP pellets were thoroughly dissolved. The stir rate was then lowered to about 50 rpm until all small bubbles were dispelled. The mixture was then put onto a glass slide and tape-cast on top of a room temperature platform. The tape

Table 3.4: PVDF-HFP Membranes Prepared in DMSO

Sample	PVDF-HFP (g)	DMSO (g)	Method	Extraction Solvent
15	1.0134	4.0570	5	Water
16	1.0018	4.0079	5	Ethanol

casting was done by pulling the tape-casting knife backwards over the entire slide while the slide was held in a fixed position. Method 5 was used to freeze-cast the sample, where the sample was placed on top of an aluminum block at -20°, such that one end of the slide rested on the cold finger and the other rested on a Teflon spacer (Figure 3.3a). Two different extraction solvents were then tested, water and ethanol. After freeze-casting, the membranes were placed in water or ethanol baths at 4°C overnight, then removed and washed with ethanol before being left to dry in air for 24 hours. The membranes were then cut so that their cross-sections could be imaged using SEM. This was done by immersing them in liquid nitrogen until they were brittle and applying pressure with a pre-chilled razor blade.

Chapter 4

RESULTS

4.1 Method for Fabrication of PVDF-HFP Membranes in $DMSO_2$

A method was developed for the fabrication of PVDF-HFP membranes in $DMSO_2$, which combined high-temperature tape casting and bidirectional freeze casting into a single step (Section 3.1, Figure 3.1). Four variations (Methods 1-4) were tested in order to understand how to optimize the setup to achieve uniform PVDF-HFP membranes with through-thickness, vertically aligned submicron pores. Here the findings for each method are summarized. For figures, HOT indicates the side which was not in contact with the cold surface during bidirectional freeze-casting.

4.1.1 Method 1

Tape-casting temperatures of 160°C and 130°C were tested using Method 1 (Figure 3.1a, Table 3.1). It was found that tape casting at 160°C caused significant evaporation of $DMSO_2$ from the sample before the freeze-casting step, causing large regions of the resulting membrane to form a clear PVDF-HFP film. In addition, the high evaporation rate seemed to cause nonuniformities in the viscosity of the dope solution, occasionally causing the tape-casting knife to get stuck. Tape casting at a lower temperature of 130°C lessened the evaporation of $DMSO_2$ from the sample. The resulting membrane had a nonuniform appearance, with some regions being translucent with a visible underlying structure and other regions being opaque (Figure 4.1). Accordingly, samples were collected from both the translucent and opaque regions. The cross-sectional microstructure observed in the translucent region is shown in Figure 4.2. The observed microstructure for samples collected in this region showed smooth-walled pores which were about 5 μm in diameter, with varying pore orientations which have intersecting paths. The cross-sectional microstucture of samples collected from the opaque regions is shown in Figure 4.3. In this region, directionally aligned, through thickness, smooth-walled pores which were 2 μm to 3 μm in diameter were observed.

4.1.2 Method 2

In Method 2, high-temperature tape casting and bidirectional freeze casting were performed simultaneously, as the sample was transferred onto a cold plate while it

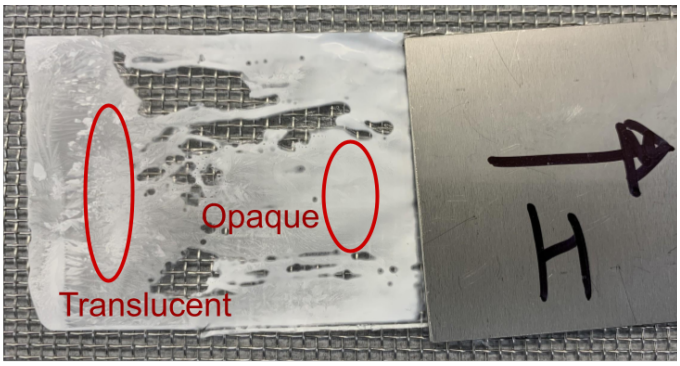

Figure 4.1: Opaque and translucent regions of PVDF-HFP membrane made using Method 1 with tape-casting temperature of 130°C. The arrow indicates the direction of the freezing front.

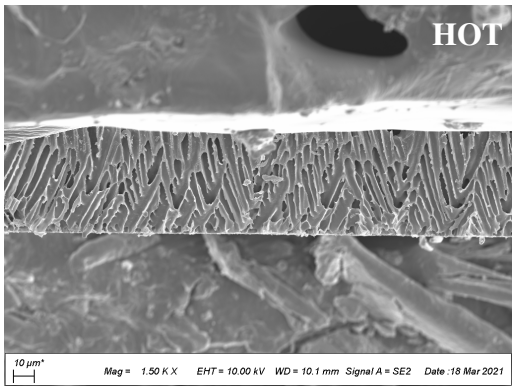

(a) Two pore alignment directions.

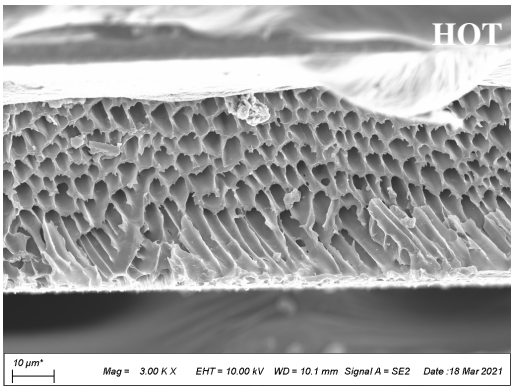

(b) In-plane and out-of-plane pores.

Figure 4.2: Cross-sectional SEM images of the translucent part of PVDF-HFP membrane made using Method 1 with tape-casting temperature of 130°C.

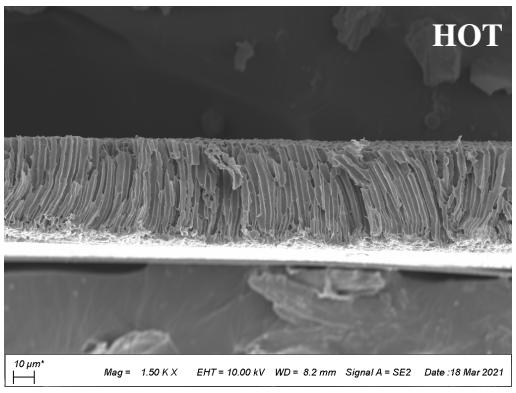

(a) Smooth-walled pores.

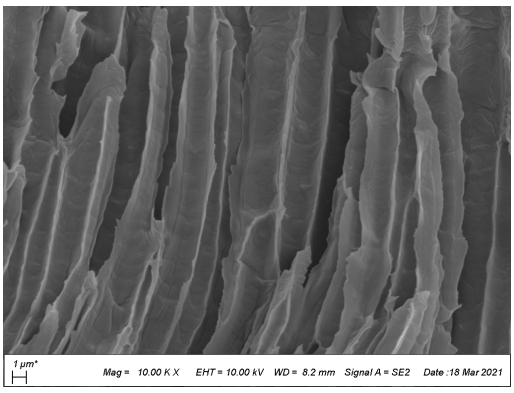

(b) Section of (a) at higher magnification.

Figure 4.3: Cross-sectional SEM images of the opaque part of PVDF-HFP membrane made using Method 1 with tape-casting temperature of 130°C.

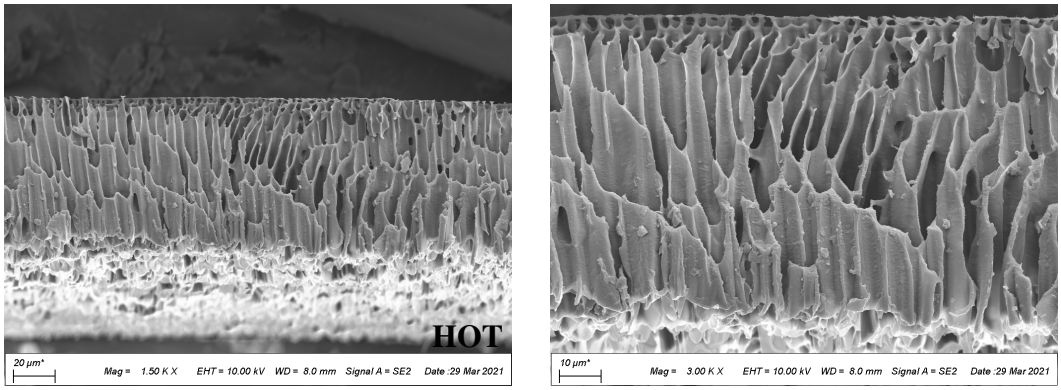

(a) Vertically aligned pores. (b) Section of (a) at higher magnification.

Figure 4.4: Cross-sectional SEM images of PVDF-HFP membrane made using Method 2.

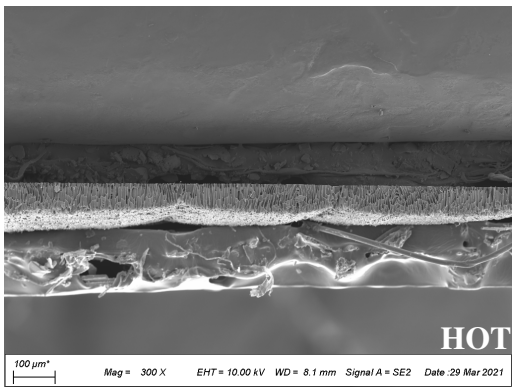

Figure 4.5: Variations in thickness for PVDF-HFP membrane made using Method 2.

was being tape-cast from a high temperature system (Figure 3.1b). This method greatly helped to reduce $DMSO_2$ evaporation across the sample and resulted in easier tape-casting. Microstructures with vertically aligned, through-thickness pores which were 5 μm to 7 μm in diameter were obtained using this method (Figure 4.4). The microstructures were observed to be uniform throughout the sample. However, somewhat periodically occurring irregularities in the sample thickness were observed in the sample (Figure 4.5).

4.1.3 Method 3

In Method 3, the tape-casting knife was positioned at the center of the heated aluminum block to prevent "tipping" of the sample as it was pushed onto the room temperature steel plate during the freeze-casting step (Figure 3.1c). The thickness of the resulting sample was observed to be uniform. The samples fabricated using

Method 3 were found to have varying microstructure across the membrane, with several regions showing differences in pore alignment direction, dendritic pore structures, and isotropic pores. Throughout the sample, pore diameters approaching 1 μm were observed. Figure 4.6 shows a microstructure with pores of approximately 1 μm diameter, which are observed to have some directional alignment. Figure 4.6b shows the dendritic pore structures that were observed.

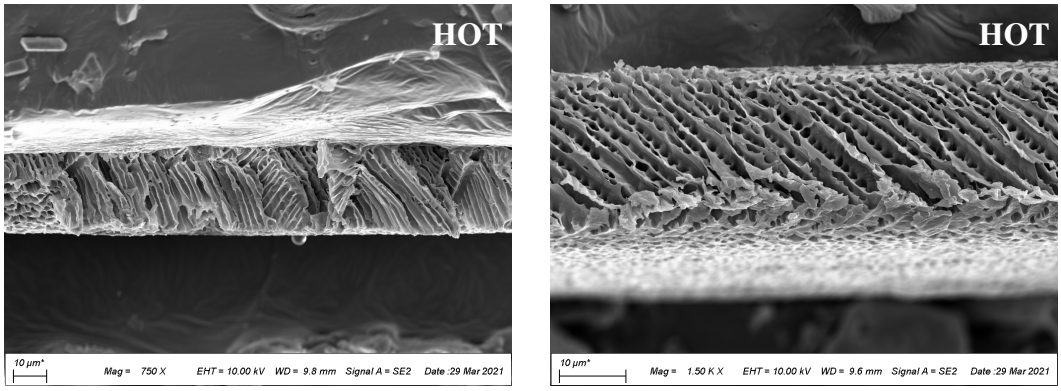

(a) Variations in alignment direction. (b) Dendritic pores.

Figure 4.6: Cross-sectional SEM images of PVDF-HFP membrane made using Method 3.

4.1.4 Method 4

In Method 4, the tape-casting knife was positioned at the center of the heated aluminum block, and the sample was pushed onto an aluminum block during the freeze-casting step rather than a steel plate (Figure 3.1d). Samples fabricated using this method were found to have an highly disordered and dendritic pore structure with pore diameter approaching 1 μm.

4.2 PVDF-HFP Membranes Prepared in DMSO and Dioxane Cosolvents

PVDF-HFP membranes were prepared in 7:3 (by weight) and 1:1 (by weight) DMSO:dioxane cosolvent mixtures. Due to differences in the melting point depression depending on the cosolvent ratio, two different methods were used for freeze-casting. The membrane which was prepared in 7:3 DMSO:dioxane cosolvents was freeze-cast using the air wedge method (Figure 3.3a) on top of an aluminum cold finger which was cooled to -25°C. The resulting membrane had a spherulitic microstructure (Figure 4.7). The membrane prepared in a 1:1 DMSO:dioxane cosolvent mixture was freeze-cast using the air wedge method on top of an aluminum boat which was lowered into a liquid nitrogen bath (Figure 3.3b), until the bottom of the boat was in contact with (or very close to) the surface of the bath. When

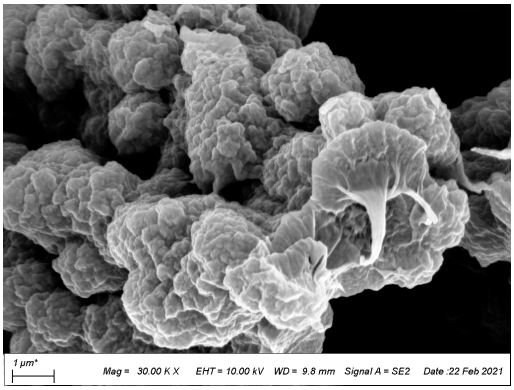

Figure 4.7: Spherulitic microstructure observed in PVDF-HFP membrane prepared in 7:3 DMSO:dioxane cosolvents.

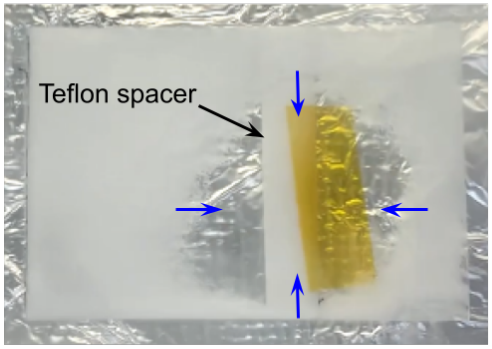

Figure 4.8: Multiple freezing fronts observed while freeze casting PVDF-HFP membrane prepared in 1:1 DMSO:dioxane cosolvents are shown with blue arrows.

using this method, rather than a single freezing front originating on the bottom of the wedge and travelling up the wedge, multiple freezing fronts were observed to originate on each edge of the glass slide and travel towards the center of the sample (Figure 4.8). The resulting microstructure showed a very irregular and nonuniform collapsed pore structure. SEM images for this method were not included because of its undesirable pore structure.

4.3 PVDF-HFP Membranes Prepared in DMSO and $DMSO_2$ Cosolvents

PVDF-HFP membranes were prepared in 1:1 DMSO:$DMSO_2$ cosolvents using Method 3 (Figure 3.1c), but with differing freeze-casting temperatures.

One of the membranes was freeze-cast by pushing the glass slide onto a room temperature steel plate, as had been done for the samples prepared in $DMSO_2$. This membrane was found to have vertically aligned pores with pore diameters of

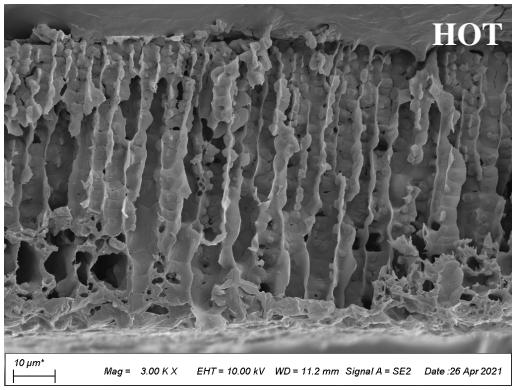

(a) Pore structure of membrane freeze-cast by pushing onto a room-temperature steel plate.

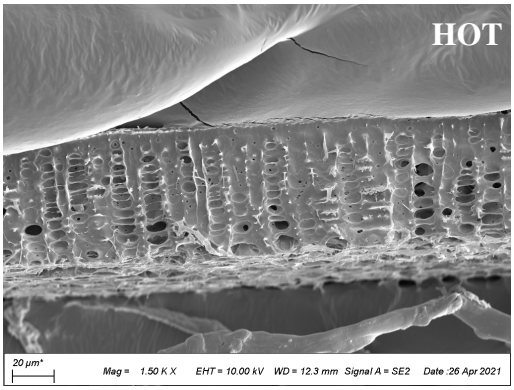

(b) Pore structure of membrane freeze-cast by pushing onto a steel plate pre-chilled in liquid nitrogen.

Figure 4.9: Cross-sectional SEM images of PVDF-HFP membranes prepared in 1:1 DMSO:$DMSO_2$ cosolvents.

approximately 3 μm, as well as PVDF-HFP spherulites which were distributed on the pore walls (Figure 4.9a). The other membrane was freeze-cast by pushing onto a steel plate that was pre-chilled in liquid nitrogen. The resulting microstructure consisted of large, vertical, dendritic pores with diameters of approximately 7 μm to 10 μm (Figure 4.9b).

4.4 PVDF-HFP Membranes Prepared in DMSO

PVDF-HFP membranes prepared in DMSO were found to have an isotropic pore microstructure, with pore diameters approaching 1 μm. SEM images for this method were not included because of its undesirable pore structure.

Chapter 5

DISCUSSION AND FUTURE DIRECTIONS

5.1 High-Temperature Tape-Casting Method

The general high-temperature casting method consisted of tape casting on top of an aluminum block which was pre-heated by partially submerging it in a silicone oil bath. Bidirectional freeze casting was then performed by gradually transferring the sample from the high-temperature surface of the aluminum block to a low-temperature surface, inducing the crystallization of the solvent and giving the porous structure. Four variations of this high-temperature tape-casting method were tested using the PVDF-HFP in $DMSO_2$ polymer-solvent system to see if they would give the desired membrane microstructure of vertically aligned, nontortuous, submicron pores.

While none of the methods succeeded in obtaining a submicron pore size, Method 2 succeeded in yielding vertically aligned, nontortuous pores uniformly throughout the sample. Methods 1 and 3 succeeded in producing pores approaching diameters of 1 μm with some directional alignment, though the pore orientations and even the pore morphologies were found to be nonuniform for these methods, appearing cellular in some parts of the sample and dendritic in others. Therefore, pending some modifications to further reduce the pore size of the obtained membranes, Method 2 shows the most promise as a high-temperature tape-casting method for fabricating polymer membranes with the desired pore morphology. The results from Methods 1 and 3 may provide insight into how to improve Method 2 to obtain smaller pore sizes.

The following subsections detail what we found to be important considerations when using the high-temperature tape-casting method, particularly for the future use of Method 2 to make polymer membranes with vertically aligned, nontortuous, and submicron pores.

5.1.1 Evaporation of the Crystallizable Solvent

The evaporation of the crystallizable solvent out of the sample after tape casting and before freeze casting presented a challenge when producing porous membranes.

While performing Methods 1, 3, and 4, the freezing front was found to avoid some regions of the sample during the bidirectional freeze-casting step. These regions would later form clear films rather than the translucent white films representative of a porous microstructure (Figure 4.1). These observations suggest that there was not enough $DMSO_2$ in those regions to observe a freezing front. In all three of these methods, after being tape-cast, the membrane remained on the heated aluminum block for some time before being freeze-cast, so that relatively large amounts of $DMSO_2$ were able to evaporate out of the tape-cast sample. In Method 2, however, the tape-casting and freeze-casting steps were performed simultaneously, reducing the surface area of the dope solution during the time that it was on the heated aluminum block and therefore minimizing the evaporation of $DMSO_2$ out of the sample.

On the other hand, pore diameters approaching 1 μm were achieved using Methods 1 and 3, while Method 2 gave pore diameters of approximately 5 μm to 7 μm. Method 4 is not considered here because the observed pores were not of the desired morphology. The smaller pore size obtained using Methods 1 and 3 may have also been a result of the rapid evaporation of $DMSO_2$ from the membranes after tape-casting. It is possible that the increased viscosity of the dope solution due to higher PVDF-HFP concentration restricted the crystallization of $DMSO_2$, decreasing the pore size [3]. In support of this idea, while fabricating PVDF membranes in $DMSO_2$ using the TIPS method, Liang et al. found that the pore size and surface porosity dramatically decreased with increased PVDF concentration [3]. In the past, it has been difficult to prepare dope solutions with PVDF-HFP concentrations higher than 20 wt% due to their high viscosities. Nevertheless, it may be worthwhile to look into methods for increasing the PVDF-HFP concentration, either during the solution preparation step or during tape casting itself.

5.1.2 Alignment of Tape-casting and Freeze-casting Surfaces

When tape casting using Method 2, alignment of the tape-casting and freeze-casting surfaces was found to be crucial to obtaining membranes with uniform thickness. Figure 4.5 shows variations in sample thickness that were likely a result of the glass slide "tipping" as the sample was pushed from the heated aluminum block onto the room temperature steel plate, due to the misalignment between the two. The periodic variations in sample thickness may have been due to inconsistencies in the pushing force, which probably had a vertical component, or vibrations in the

steel plate. One challenge that was encountered was the task of adjusting the room temperature steel plate to be perfectly flush with the top of the heated aluminum block. Since the membrane is only a few tens of microns thick, this was impossible without special equipment, since any small misalignment would have a marked effect on the obtained membranes. For Method 2 to be viable, a way to align these surfaces without sacrificing the horizontal temperature gradient will be necessary.

5.1.3 Influence of Horizontal and Vertical Temperature Gradients

In unidirectional freeze-casting, a single vertical temperature gradient is used to control the direction of solvent crystal growth, whereas in bidirectional freeze-casting, an additional horizontal temperature gradient is added to promote ordered nucleation of the solvent crystals. The two gradients are often considered separately, but can also be thought of as a single two-dimensional gradient (i.e. a heat map). Therefore, the horizontal gradient should also have some effect on the range of orientations at which crystals can grow.

In this work, Method 2 was found to give straight, completely vertical pores, while Methods 1 and 3 gave pores which were slanted and curved. Such discrepancies in pore orientations resulting from different bidirectional freeze-casting methods have also been found in the literature. Using the bidirectional freeze-casting method shown in Figure 2.4, in which the horizontal temperature gradient was obtained by addition of a coolant into a reservoir, Liang et al. obtained membranes with extremely vertical pores using several different recrystallizable solvents [4]. In this method, the coolant which induced the ordered nucleation of solvent crystals was in contact with both sides of the mold, increasing the uniformity of the horizontal temperature gradient across the thickness of the membrane. Meanwhile, Kim et al. used the bidirectional freeze-casting method shown in Figure 2.5, in which the horizontal temperature gradient was achieved by moving the sample at a fixed rate towards a liquid nitrogen reservoir, to yield membranes with slanted pores [1]. In this method, the liquid nitrogen reservoir was located underneath the membrane, so that the horizontal temperature gradient was strongest on the bottom surface of the membrane and weakest on the top surface. The authors attribute the slanted structure of the resulting pores to the high thermal conductivity of the solvent reducing the temperature gradient in the vertical direction. However, it may also be the case that the uniformity of the horizontal temperature gradient during the freezing process has a strong effect on the final pore alignment.

Analogously, in Method 2, the membrane was heated from above and below by the tape-casting knife and aluminum block, respectively, just before it was transferred to the room temperature steel plate, increasing the uniformity of the horizontal temperature gradient across the thickness of the membrane. In this way, the freeze-casting process was similar to the one used by Liang et al., and both of these methods obtained completely vertical pores. In Methods 1 and 3, however, only the bottom surface of the membrane was heated by the aluminum block before it was transferred to the room temperature steel plate, where the bottom surface was cooled. Thus, in these methods the thermal gradient is again strongest on the bottom surface of the membrane and weakest on the top surface, similar to the method used by Kim et al. Therefore, the uniformity of the horizontal temperature gradient across the thickness of the sample during bidirectional freeze casting seems to have significant effects on the pore orientation. It may be the case that a more uniform horizontal temperature gradient across the sample thickness restricts the range of angles at which solvent crystals can grow, leading to more vertical pores. A larger literature search would have to be conducted to see whether this theory actually explains the difference in pore orientations resulting from various bidirectional freezing-casting methods.

In addition, the vertical temperature gradient may offer another potential solution for obtaining smaller pore sizes. Solidification theory suggests that the spacing between primary dendrites can be reduced by increasing the vertical temperature gradient [6]. This is another avenue worth investigating for further decreasing the pore sizes of membranes fabricated using Method 2.

5.1.4 Rate of Transfer to Freeze-Casting Surface

The rate of transfer from the tape-casting surface to the freeze-casting surface was not controlled in our experiments, since this was done by using a spatula to push the sample across the tape-casting and freeze-casting surfaces by hand. Future work will have to be done to optimize the transfer rate. However, it is worth noting that Method 2 is the most amenable to controlling the transfer rate. Methods 1 and 3 are less suitable, as they must be transferred quickly to the steel plate because of the high rate of evaporation of $DMSO_2$ from the tape-cast samples.

5.2 Solid-Liquid Phase Separation of PVDF-HFP

The PVDF-HFP membrane which was prepared in 7:3 (by weight) DMSO:dioxane cosolvents had a spherulitic microstructure (Figure 4.7), which can be attributed to the high concentration of PVDF-HFP in the dope solution (15 wt%). At high

enough polymer concentrations, solid-liquid phase separation can occur upon cooling, causing the polymer to crystallize out of the dope solution (Figure 2.1). In contrast to the 15 wt% which was used here, Kim et al. prepared membranes using only 7 wt% PVDF in a cosolvent mixture with the same DMSO:dioxane ratio [1]. For further investigation into the cosolvent method, it may be worthwhile to repeat the experiment with lower polymer concentrations.

The membranes which were prepared in 1:1 DMSO:$DMSO_2$ cosolvents provide some insight into how PVDF-HFP crystallization may come into play during bidirectional freeze-casting. The difference between the preparation of the two samples occurred during the freeze-casting step, where one was pushed onto a room-temperature steel plate, and the other was pushed onto a steel plate which was pre-chilled in liquid nitrogen. This difference resulted in two very different pore morphologies. The membrane pushed onto a room-temperature steel plate had vertically aligned pores with PVDF-HFP spherulites distributed on its pore walls (Figure 4.9a). It is clear from looking at the microstructure of this sample that both polymer crystallization and solvent crystallization were occurring simultaneously, demonstrating that crystallization of PVDF-HFP and crystallization of the solvent can be competing processes in determining the final microstructure. In other words, increasing the rate of crystallization of the solvent could drive the membrane towards having vertically oriented pores, while decreasing the rate of crystallization of the solvent could cause the spherulitic microstructure to dominate. Supporting this theory, PVDF-HFP spherulites were not observed in the microstructure of the membrane which was pushed onto a steel plate pre-chilled in liquid nitrogen (Figure 4.9b). It seems that decreasing the freeze-casting temperature promoted the crystallization of the solvent over the crystallization of PVDF-HFP, indicating that for this polymer-solvent system, the temperature sensitivity of the solvent crystallization rate was higher than that of polymer crystallization rate. Increasing the solvent crystallization rate by lowering the freeze-casting temperature may therefore be a method to avoid the formation of spherulites when preparing PVDF-HFP membranes from dope solutions with higher concentration of PVDF-HFP.

Chapter 6

CONCLUSION

In this work we propose a high-temperature tape-casting and bidirectional freeze-casting method for fabricating PVDF-HFP membranes in $DMSO_2$. Using this method, PVDF-HFP membranes through-thickness, vertically aligned submicron pores which were 5 μm to 7 μm in diameter were obtained. The pore morphology and membrane thickness were found to be uniform. This method is particularly advantageous because the tape-casting and freeze-casting steps are performed simultaneously, reducing the surface area of the dope solution during its time on the heated aluminum block and therefore minimizing the evaporation of DMSO2 out of the sample. This method is scalable and lends itself to greater control over the transfer rate from the tape- to freeze- casting surfaces during bidirectional freeze-casting, which may be the subject of future work. It also offers greater uniformity of the horizontal temperature gradient across the thickness of the sample. To the end of developing a battery separator, however, the pore size obtained using this method is too large. Submicron pore sizes may be achieved by increasing the polymer concentration in the dope solution or increasing the thermal gradient in the vertical direction during the freeze-casting step. Future work should also entail optimization of the setup to ensure perfect alignment of the tape-casting and freeze-casting surfaces and determination of the ideal transfer rate between the surfaces during the freeze-casting step.

Lastly, the occasional role of PVDF-HFP crystallization during bidirectional freeze casting was discussed. Notably, it was found that PVDF-HFP crystallization and solvent crystallization can be competing processes during formation of the membrane. The crystallization rate of the solvent may therefore be an important consideration in future work, particularly if higher polymer concentrations are to be used in the dope solution.

BIBLIOGRAPHY

[1] Byoung Soo Kim and Jonghwi Lee. Pore size reduction in directional crystallization processing of porous polymeric membranes. *Journal of nanoscience and nanotechnology*, 13(3):2276–2283, 2013.

[2] Jeong F Kim, Ji Hoon Kim, Young Moo Lee, and Enrico Drioli. Thermally induced phase separation and electrospinning methods for emerging membrane applications: A review. *AIChE Journal*, 62(2):461–490, 2016.

[3] Hong-Qing Liang, Qing-Yun Wu, Ling-Shu Wan, Xiao-Jun Huang, and Zhi-Kang Xu. Polar polymer membranes via thermally induced phase separation using a universal crystallizable diluent. *Journal of membrane science*, 446: 482–491, 2013.

[4] Hong-Qing Liang, Ke-Jia Ji, Li-Yun Zha, Wen-Bing Hu, Yang Ou, and Zhi-Kang Xu. Polymer membranes with vertically oriented pores constructed by 2d freezing at ambient temperature. *ACS applied materials & interfaces*, 8 (22):14174–14181, 2016.

[5] Hansan Liu and Katherine Faber. Advanced multifunctional battery separators for novel liquid electrolytes. *DOE STTR Phase I, Topic# 19a*, 2020.

[6] SM Miller, X Xiao, and KT Faber. Freeze-cast alumina pore networks: Effects of freezing conditions and dispersion medium. *Journal of the European Ceramic Society*, 35(13):3595–3605, 2015.

[7] Maninpat Naviroj, Peter W Voorhees, and Katherine T Faber. Suspension- and solution-based freeze casting for porous ceramics. *Journal of Materials Research*, 32(17):3372–3382, 2017.

[8] Elsa A Olivetti, Gerbrand Ceder, Gabrielle G Gaustad, and Xinkai Fu. Lithium-ion battery supply chain considerations: analysis of potential bottlenecks in critical metals. *Joule*, 1(2):229–243, 2017.

[9] Vince Wu and Claire Kuo. Technical report for talos tech for doesttr2o532-subo1. Technical report, Caltech, November 2020.

[10] Chongyin Yang, Ji Chen, Xiao Ji, Travis P Pollard, Xujie Lü, Cheng-Jun Sun, Singyuk Hou, Qi Liu, Cunming Liu, Tingting Qing, et al. Aqueous li-ion battery enabled by halogen conversion–intercalation chemistry in graphite. *Nature*, 569(7755):245–250, 2019.